Deep Sequencing Analysis of Aptazyme Variants Based on a Pistol Ribozyme

Deep Sequencing Analysis of Aptazyme Variants Based on a Pistol Ribozyme

Shungo Kobori, Kei Takahashi, and Yohei Yokobayashi*

Nucleic Acid Chemistry and Engineering Unit, Okinawa Institute of Science and Technology Graduate University, Onna, Okinawa 904 0495, Japan

S *Supporting Information*

ABSTRACT: Chemically regulated self-cleaving ribozymes, or aptazymes, are emerging as a promising class of genetic devices that allow dynamic control of gene expression in synthetic biology. However, further expansion of the limited repertoire of ribozymes and aptamers, and development of new strategies to couple the RNA elements to engineer functional aptazymes are highly desirable for synthetic biology applications. Here, we report aptazymes based on the recently identified self-cleaving pistol ribozyme class using a guanine aptamer as the molecular sensing element. Two aptazyme architectures were studied by constructing and assaying 17 728 mutants by deep sequencing. Although one of the architectures did not yield functional aptazymes, a novel aptazyme design in which the aptamer and the ribozyme were placed in tandem yielded a number of guanine-inhibited ribozymes. Detailed analysis of the extensive sequence-function data suggests a mechanism that involves a competition between two mutually exclusive RNA structures reminiscent of natural bacterial riboswitches.

KEYWORDS: *RNA engineering, ribozyme, aptamer, aptazyme, high-throughput sequencing, riboswitch*
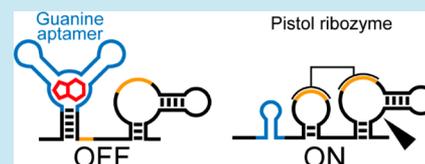
The combination of an aptamer (DNA or RNA) and a nucleic acid enzyme (deoxyribozyme or ribozyme) to create chemically regulated aptazymes has long attracted the attention of chemists as a model of allosteric enzymes as well as for applications in biosensing.[1,2] In synthetic biology, aptazymes based on RNA aptamers and self-cleaving ribozymes have proven to be useful for chemical regulation of gene expression in living cells and in cell-free translation systems.[3] While an aptazyme itself simply self-cleaves in the presence or absence of its cognate aptamer ligand, integration with regulatory RNA elements such as ribosome-binding site, 3′-untranslated region (UTR) in mRNA, tRNA, or pri-miRNA enables chemical control of gene expression in a variety of cellular and genetic contexts.[3] However, the variety of aptamers and self-cleaving ribozymes, and the strategies to link the two RNA elements to engineer aptazymes have been rather limited. To date, aptamers that bind theophylline,[4−7] tetracycline,[8,9] thiamine pyrophosphate,[10,11] and guanine[12,13] have been used to construct aptazymes to regulate gene expression in living cells and in cell-free translation systems. While aptazymes based on the hammerhead ribozyme scaffold are the most common,[4−12] aptazymes based on other ribozyme classes such as hepatitis delta virus (HDV) ribozymes[13] and twister ribozymes[14] have been reported. Availability of ribozymes with different secondary and tertiary structures, biochemical properties, and sequence requirements at the cleavage site benefits diverse applications of aptazymes. More importantly, virtually all of these aptazymes share a common architecture in which a ligand-binding aptamer is inserted within a stem-loop of a ribozyme scaffold. In most cases, the mechanism of allosteric regulation of ribozyme activity has been attributed to either stabilization or destabilization of the local stem structure upon aptamer-ligand binding.[1] Further expansion of the repertoire of aptamers and ribozymes as well as development of new design strategies for engineering aptazymes should lead to increased engineering flexibility and broader applications in synthetic biology.

In this report, we describe the first examples of aptazymes based on the recently discovered pistol ribozyme motif.[15,16] Furthermore, a novel aptazyme architecture in which an aptamer and a ribozyme are linked in tandem, rather than the conventional design in which an aptamer is inserted within a ribozyme, is presented. *In vitro* cotranscriptional cleavage efficiencies of 16 384 aptazyme mutants in the presence and absence of guanine were assayed using the deep sequencing method we recently developed[17,18] with a few modifications that increase its generality. We identified a number of guanine-inhibited aptazymes under the reaction conditions and observed key design criteria of the new aptazyme architecture.

■ RESULTS AND DISCUSSION

Pistol ribozymes are characterized by three conserved stems P1−P3, a pseudoknot between the hairpin loop of P1 and the internal loop connecting P2 and P3, and a linker that connects P1 and P2.[15,16] The secondary structure depicted in Figure 1a based on the computational analysis of the ribozyme variants was recently confirmed by crystallography.[19,20] We designed two aptazyme libraries based on a pistol ribozyme variant found in *Alistipes putredinis*[16] and a guanine aptamer derived from the
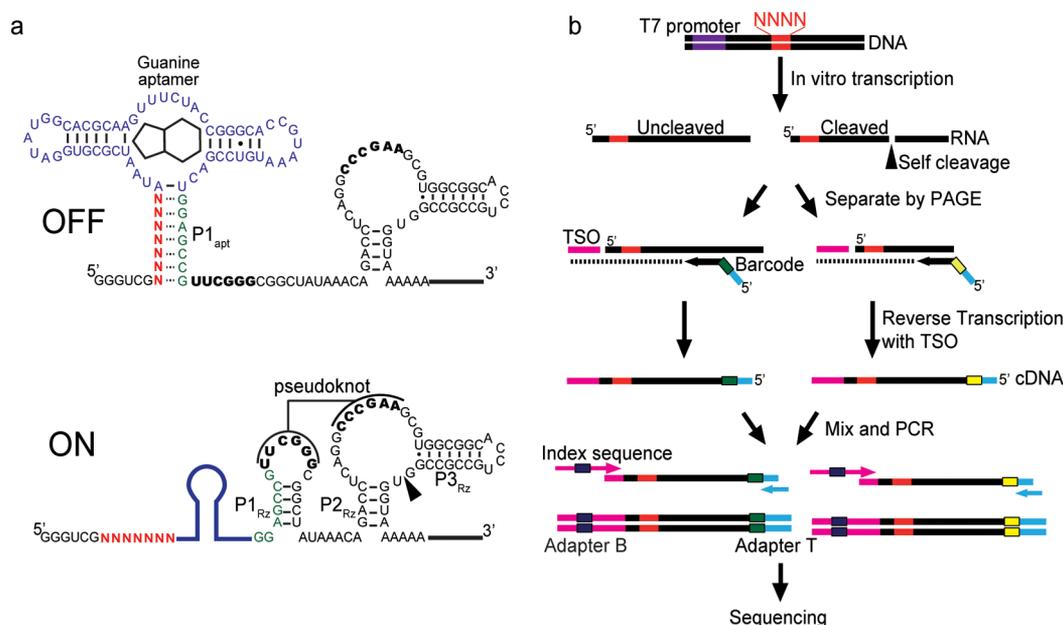
Figure 1. Aptazyme design and library construction. (a) Aptazyme library Lib-2: the guanine aptamer (blue) and the ribozyme were fused in tandem. Seven degenerate bases (N, red) were inserted to the 5′ side of the aptamer. It was envisioned that these bases could form a putative aptamer stem (P1$_{apt}$) in the presence of guanine resulting in disrupted ribozyme structure and activity (OFF), but withdrawal of guanine would restore the ribozyme structure and activity (ON). (b) Outline of the procedures for deep sequencing library preparation.

riboswitch in the *xpt-pbuX* operon of *Bacillus subtilis*.[21] In library Lib-1, the guanine aptamer was inserted in P3 of the ribozyme via three, four, or five randomized nucleotides (Supporting Information, Figure S1a). The rationale for this library design was that the aptamer–ligand interaction would modulate the local structure of the ribozyme close to the cleavage site, therefore its activity. The second library (Lib-2) placed the guanine aptamer directly upstream of the pistol ribozyme, while randomizing seven nucleotides adjacent to the 5′ end of the aptamer (Figure 1a). At first glance, randomizing nucleotides far away from the ribozyme may appear counter-intuitive for aptazyme discovery. However, we postulated that the bases targeted for mutagenesis could potentially participate in the P1 stem of the guanine aptamer (P1$_{apt}$) in the presence of the ligand, and if that were to occur, it would interfere with the formation of the conserved P1 stem of the pistol ribozyme (P1$_{Rz}$), rendering it inactive (Figure 1a). This aptazyme architecture was partly inspired by the natural riboswitches (including the purine riboswitches) whose aptamer and downstream gene regulatory RNA structures are mutually exclusive and cannot coexist.[22] Stability of the putative P1$_{apt}$ stem relative to that of P1$_{Rz}$ was anticipated to be a key design parameter. Therefore, we randomized seven nucleotides with an expectation that the library covers P1$_{apt}$ with varying stability, some of which could lead to ligand-dependent modulation of the ribozyme activity.

We assayed *in vitro* cotranscriptional cleavage efficiencies of all variants in the libraries by applying the high-throughput ribozyme assay strategy based on deep sequencing we recently developed (Figure 1b).[17,18] Each aptazyme library was prepared as a mixture of dsDNA templates for *in vitro* transcription by T7 RNA polymerase. After 3 h of transcription reaction at 37 °C either with or without guanine, the uncleaved transcript and the cleaved fragment that contains the randomized nucleotides were isolated separately by polyacrylamide gel electrophoresis (PAGE). The two fragments were separately reverse tran-

scribed using a primer that contains an identifier sequence (barcode) that indicates whether the transcript was cleaved or not cleaved. The reverse transcription reaction also added a partial adapter sequence that is necessary for deep sequencing to the 3′ end of the cDNA by the template-switching mechanism.[23] The cDNAs were combined into a single tube, preserving the relative quantities of the cleaved and uncleaved transcripts, and further amplified by PCR to add complete adapter sequences and an index sequence to indicate the presence or absence of the ligand. Deep sequencing of the resulting samples yielded, on average, approximately 2400 to 7200 reads per variant depending on the library (Table S2). For each mutant, fraction cleaved (FC) was calculated as follows:

$$FC = n_c / (n_c + n_{unc})$$

where n_c and n_{unc} are the read counts of the cleaved and uncleaved fragments, respectively.

In this work, we also addressed a significant technical limitation in our previously reported procedures which required the self-cleavage site to occur upstream of the mutagenized bases.[17,18] This limitation existed because determination of the cleavage status of each transcript was made based on direct sequencing of the cleavage site. We circumvented this restriction by physical separation of the cleaved and uncleaved fragments and subsequent attachment of unique barcodes to record the cleavage status during reverse transcription. This allows significant flexibility in the architecture of the aptazymes to which one can apply this method.

Analysis of the deep sequencing data yielded FC values of all library variants in the presence and absence of guanine. Most of the variants in Lib-1 showed low cleavage activity and did not yield potentially promising aptazyme candidates (Figure S1) suggesting that insertion of a large aptamer in P3 is disruptive for ribozyme folding. Therefore, this library was not pursued further. However, it cannot be concluded that insertion of an aptamer within P3 or elsewhere in a pistol ribozyme cannot

yield functional aptazymes based on this observation alone. FC values of all 16 384 (= 4^7) variants from Lib-2 in the presence and absence of guanine were plotted as shown in Figure 2. An
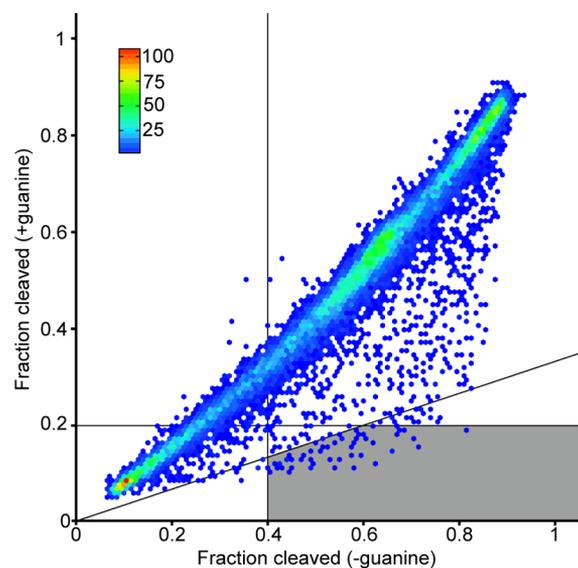

Figure 2. Ribozyme activity profile (fraction cleaved) of 16 384 aptazyme variants in Lib-2 in the presence (500 μM) and absence of guanine. The shaded region includes 53 guanine-inhibited aptazymes that meet the performance criteria discussed in the text.

overwhelming majority of the variants populate the region near the identity line ($y = x$) indicating that their cleavage efficiencies do not depend on guanine which is not surprising considering the distance of the randomized region from the ribozyme. However, there is a clear distribution of variants scattered below the identity line cluster which indicates the presence of few variants whose cleavage efficiencies are negatively affected by guanine.

To validate the deep sequencing derived data, 10 variants were individually prepared and assayed under the same conditions by conventional gel electrophoresis. FC values obtained by PAGE agreed well with the corresponding values obtained by deep sequencing (Figure 3 and Figure S2), as has been the case in our previous reports.[17,18] Modulation of ribozyme activity by guanine was also confirmed with the variants identified from our deep sequencing results, with up to 8.6-fold repression of FC in the presence of guanine by PAGE assay (Table 1 and Figure S2).

The comprehensive sequence-function data set (Supporting Information, data set) acquired by our deep sequencing assay allows us to explore the design principles of the aptazyme architecture without the iterative process of mutagenesis and functional assay. Our rationale for the library design was to cover a sufficient range of the stability of the putative $P1_{apt}$ stem. This meant that the variant that could form the most stable $P1_{apt}$ stem by perfect Watson−Crick (WC) base pairing at all randomized positions (i.e., CGGCUCC) should exhibit a diminished self-cleavage activity even in the absence of the ligand. Indeed, the variant CGGCUCC showed FC values of 0.071 and 0.095 in the presence and absence of guanine, respectively (Table 1), suggesting that the sequence space explored in the library covers a sufficient range of $P1_{apt}$ stability.

We then screened the variants for guanine responsive aptazymes based on the following criteria: FC in the absence
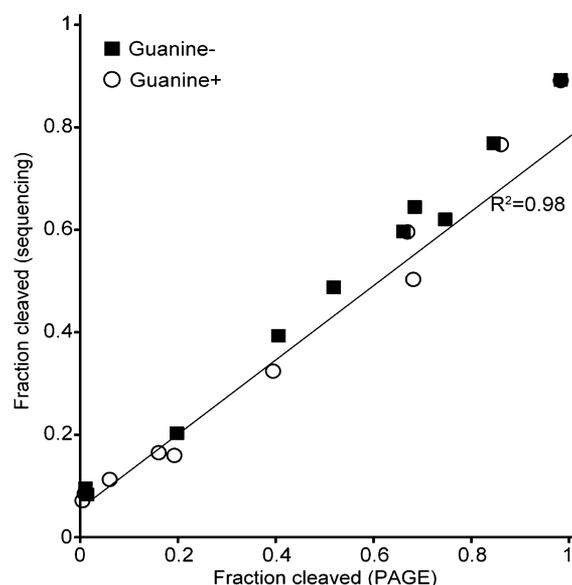

Figure 3. Correlation of FC values derived from deep sequencing and PAGE of 10 selected ribozyme variants from Lib-2. Two measurements by PAGE were performed for each variant.

Table 1. Activities of Selected Ribozyme Variants from Lib-2

sequence (5′−3′)	sequencing		PAGE	
	fraction cleaved (∓guanine)	ON/OFF ratio	fraction cleaved (∓guanine)	ON/OFF ratio
CGGCUCC	0.095/0.071	1.34	0.011/0.00[a]	n.d.
CAAGUUU	0.083/0.085	0.98	0.014/0.00[a]	n.d.
UUUUUGG	0.20/0.16	1.27	0.20/0.19	1.03
CCGGACA	0.39/0.32	1.21	0.41/0.39	1.03
AAAAUUG	0.60/0.50	1.19	0.66/0.68	0.97
CGGAUAG	0.64/0.60	1.08	0.68/0.67	1.02
CUCCAUC	0.77/0.77	1.00	0.85/0.86	0.98
AACCCAA	0.89/0.89	1.00	0.98/0.98	1.00
UCACACC	0.62/0.16	3.76	0.75/0.16	4.65
GCUAACC	0.49/0.11	4.34	0.52/0.060	8.58

[a]Cleaved RNA was not visible on the gel.

of guanine (FC−) > 0.40, FC in the presence of guanine (FC+) < 0.20, FC−/FC+ > 3.0. This resulted in 53 variants that fall in the shaded region in Figure 2 and comprise 0.32% of the 16 384 variants assayed (Table S3). Frequencies of the four bases at each position within the randomized region indicate a strong consensus (NNN[C/U]UCC) at the last four positions (Figure 4a). These bases are complementary to the opposite side of the $P1_{apt}$ sequence proximal to the aptamer, suggesting that the positions closer to the aptamer are more important for the aptazyme function. We further examined the general trend of the ribozyme activity as $P1_{apt}$ is stabilized by analyzing subpopulations of the variants with zero to seven WC base pairs proximal to the aptamer within the randomized region (Figure 4b). The FC-values maintained a high level from zero to four base pairs and progressively decreased from five to seven base pairs. This trend indicates that in this aptazyme configuration, approximately five additional WC base pairs are necessary for $P1_{apt}$ to compete with $P1_{Rz}$. Intriguingly, a qualitatively similar trend was observed for FC+ with a decrease in ribozyme activity starting at three base pairs. Taken together, the general sequence-function relationship of the aptazyme
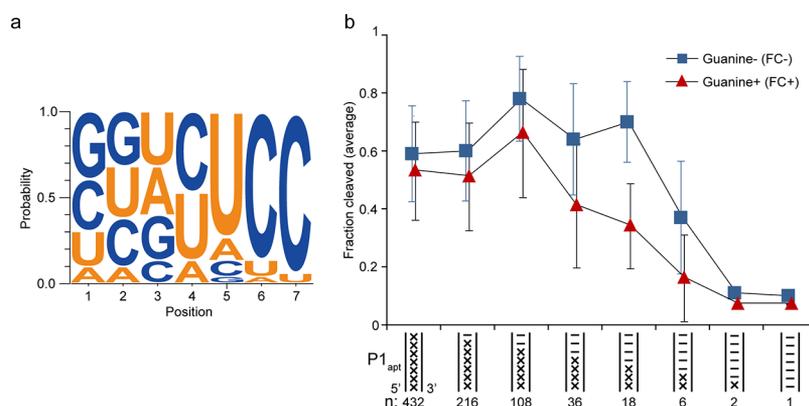
Figure 4. Sequence-function relationships of Lib-2 aptazymes. (a) Base frequencies of the degenerate bases in the 53 aptazymes discussed in the text. The figure was generated using WebLogo3.[28] (b) Average FC of Lib-2 subpopulations with different numbers of WC base pairs in $P1_{apt}$ proximal to the aptamer. "x" indicates a mismatch and "−" indicates a WC base pair (A-U/U-A or G-C/C-G). Sequences containing wobble base pairs (G-U/U-G) were excluded. N: number of variants in each $P1_{apt}$ subpopulation. The data shown are mean ± standard deviation (SD).

library supports the competition between the two mutually exclusive stems $P1_{apt}$ and $P1_{Rz}$ as depicted in Figure 1a, and that the fine-tuning of $P1_{apt}$ stability is the key criterion for the performance of the aptazymes.

Apart from aptazymes, a careful look into the sequence-function data set reveals additional insights. While the majority of Lib-2 variants do not respond to guanine, it is notable that the FC values of the ribozymes span a wide range (Figure 2). This suggests that although the randomized nucleotides are located more than 50 bases upstream of the ribozyme, they can have significant influence of the ribozyme activity. Context dependence of ribozyme activity has been implicated in some previous studies,[24,25] but sensitivity of ribozymes to the surrounding sequences has not been extensively investigated. We extracted 100 variants from Lib-2 with the lowest FC values (<0.083) (Table S4). Examination of these sequences revealed a few recurrent motifs. For example, GUUU at the last four bases was found in 11 variants. GUUU followed by AUA from the aptamer results in a stretch of nucleotides (GUUUAUA) that can form a perfect WC stem with the sequence near the linker between $P1_{Rz}$ and $P2_{Rz}$ in the ribozyme (UAUAAAC), likely interfering with the ribozyme folding (Figure S3). The variant with the lowest FC value in the library (UCUGUUU) further extends this putative stem by three base pairs (underlined) into a part of $P2_{Rz}$.

Similarly, 26 of the 100 variants with the lowest FC- values start with AGG in the randomized region (Table S4), suggesting a common mechanism that interferes with the ribozyme structure. A plausible secondary structure suggested by RNAalifold[26] is an imperfect stem formed by the AGG and the six preceding bases, GGGUCGAGG, and the 10 base sequence CCUCAGGCCC in $P2_{Rz}$ and the linker between $P2_{Rz}$ and $P3_{Rz}$, involving nine base pairs (Figure S3). These observations underscore the sensitivity of ribozyme activity to sequences quite distant from the ribozyme motif, which may need to be carefully addressed in various applications of ribozymes.

Although only two functional aptazyme variants were assayed by PAGE (Table 1) yielding ON/OFF ratios of 4.7 and 8.6, these values are comparable to those of our recently described aptazymes based on the HDV ribozyme motif (5.0 to 14.2)[17] which were shown to control gene expression in mammalian cells. Further improvement of the aptazyme performance may be possible by designing new libraries based on the insights

gained by the first library. For example, a new library that maintains the consensus sequence while randomizing additional positions may yield improved variants.

One promising application of aptazymes is to chemically control gene expression in living cells.[1,3] Although our initial goal was to develop a novel aptazyme architecture based on the new pistol ribozyme motif, a preliminary experiment was conducted to assess the activity of the *A. putredinis* ribozyme in mammalian cells in a context similar to that in our previous report.[17] Unfortunately, the results suggested that this specific ribozyme is not active enough under the assay conditions to control gene expression (data not shown). Consequently, if the final objective is to use aptazymes to control gene expression in living cells, it is important to first confirm the activity of the base ribozyme in the context of the intended application.

In summary, we used deep sequencing to acquire a comprehensive sequence-function data set of a novel aptazyme architecture based on a guanine aptamer and a pistol ribozyme arranged in tandem. Modulation of the relative stability of two mutually exclusive structures by aptamer-ligand binding resulted in allosteric regulation of ribozyme activity. This work also more than tripled the number of ribozyme assays achieved in a single deep sequencing experiment (16 384 variants in the presence and absence of guanine, or 32 768 assays) from our previous work in which we assayed all single and double mutants (10 296 assays) of a twister ribozyme.[18] The demonstrated increase in the number of ribozyme assays significantly broadens the sequence space that can be experimentally probed by our strategy. Finally, the library preparation protocol was modified so that more diverse ribozyme and aptazyme motifs can be studied by the assay strategy.

■ METHODS

Library Construction. DNA libraries used for *in vitro* transcription of aptazymes were constructed using synthetic oligonucleotides and PCR. Oligonucleotide and DNA fragment sequences are listed in Table S1. Oligonucleotides containing degenerate bases (N) were synthesized using the "hand-mix" option (equimolar mixture of all nucleotide phosphoramidites) offered by the manufacturers (IDT or GeneDesign, Inc.)

Briefly, Lib-1 was prepared by overlap PCR of the 5′ constant sequence Lib-1−5′Frag and the 3′ fragment containing the degenerate bases Lib1−3′FragN3/N4/N5 as templates and

PCR-Frag1-F1 and PCR-Frag1-R as PCR primers. Lib1−3′FragN3/N4/N5 fragments were generated by annealing and extending PCR-Frag1−1N3/N4/N5 and PCR-Frag1−2. Lib-2 was prepared by overlap PCR of the 5′ fragment containing the degenerate bases Lib2−5′Frag and the 3′ constant sequence Lib2−3′Frag as templates and PCR-Frag1-F2 and PCR-Frag1-R as PCR primers. Lib2−5′Frag was prepared by annealing and extending PCR-Frag2−1 and PCR-Frag2−2. The final PCR products were purified by DNA Clean & Concentrator-5 kit (Zymo Research) and used for *in vitro* transcription.

Sequences of the final dsDNA templates are as follows (T7 promoter sequence underlined):

Lib-1: 5′ <u>TAATACGACT CACTATA</u>GGG AGCCGTTCGG GCGGCTATAA ACAGACCTCA GGCCCGAAGC GT(**N3, N4, N5**)ATAAT CGCGTGGATA TGGCACGCAA GTTTCTACCG GGCACCGTAA ATGTCCGACT CCGCCGGTGG TAAAAAGAT CGGAA-GAGCA CACGTCT 3′

Lib-2: 5′ <u>TAATACGACT CACTATA</u>GGG TCGNNNNNNN ATAATCGCGT GGATATGGCA CGCAAGTTTC TACCGGGCAC CGTAAATGTC CGACTGGAGC CGTTCGGGCG GCTATAAACA GACCT-CAGGC CCGAAGCGTG GCGGCACCTG CCGCCGGTGG TAAAAAGAT CGGAAGAGCA CACGTCT 3′

***In Vitro* Transcription.** Lib-1 aptazymes (N3, N4, and N5) were individually transcribed *in vitro* in 100 μL reactions in the transcription buffer (40 mM Tris-HCl pH 8.0, 2 mM spermidine, 10 mM DTT, 4 mM $MgCl_2$) in the presence of a dsDNA template (10 pmol), NTPs (2 mM each), RNase Inhibitor, Murine (100 units, New England Biolabs), and T7 RNA polymerase (250 U, New England Biolabs) with or without guanine (500 μM) for 3 h at 37 °C. Upon completion of the transcription reaction, 20 U of DNase I (New England Biolabs) in 22 μL (54.5 mM Tris-HCl pH 7.6, 13.6 mM $MgCl_2$, 2.72 mM $CaCl_2$) was added and incubated on ice for 60 min. For Lib-2, the template was transcribed *in vitro* in a 115 μL reaction in the transcription buffer and T7 RNA polymerase (288 U, New England Biolabs) with or without guanine (500 μM) for 3 h at 37 °C. Subsequently, 20 U of DNase I in 24 μL (58.3 mM Tris-HCl pH 7.6, 14.6 mM $MgCl_2$, 2.92 mM $CaCl_2$) was added and incubated on ice for 60 min. The transcribed RNAs were purified by RNA Clean & Concentrator-5 kit (Zymo Research) and dissolved in 20 μL in 10 mM EDTA solution.

Isolation of RNA Fragments. Uncleaved and cleaved RNA fragments containing the randomized nucleotides were separated by denaturing PAGE (8% polyacrylamide, 8 M urea, 19:1 acrylamide:bis(acrylamide)). The bands corresponding to the fragments of interest from Lib-1 were separated as gel slices and RNAs were recovered by passive elution in 200 μL of TENa buffer (200 mM NaCl, 10 mM Tris-HCl pH 7.5, 5 mM EDTA) overnight at 4 °C followed by ethanol precipitation using Quick-Precip Plus Solution (Edge BioSystems) according to the manufacturer's instructions. The RNA fragments from Lib-2 were similarly prepared except that the RNAs were eluted from gel slices by electrophoresis (150 V, 15 min) using dialysis tubes (POR 1, SPECTRA) followed by ethanol precipitation using Quick-Precip Plus. The precipitated RNAs were dissolved in 11 μL in 10 mM EDTA solution.

Reverse transcription and template switching reactions. The purified RNA fragments (2.5 μL) were mixed with 100 pmol of an appropriate reverse transcription primer (RT-1-1, RT-1-2, RT-2-1, or RT-2-2, Table S1) and 3.17 mM each dNTPs in 5.13 μL. The solutions were heated to 72 °C for 3 min and placed on ice. A reverse transcription reaction was initiated by the addition of 250 U of Maxima H Minus Reverse Transcriptase (Thermo Fisher Scientific) and 250 pmol of TSO (Table S1) for the template switching reaction in 20.23 μL of RT buffer (79.7 mM Tris, pH 8.3, 120 mM KCl, 13.44 mM $MgCl_2$, 7.96 mM DTT, 1 U/μL of RNase Inhibitor, Murine, 12.4% PEG). The reaction was quenched by the addition of 1.25 μL of NaOH solution (5 M) and heat (95 °C for 5 min). The cDNAs were first cleaned by Oligo Clean & Concentrator kit (Zymo Research) and purified by denaturing PAGE (8% polyacrylamide, 8 M urea, 19:1 acrylamide:bis(acrylamide)). The gel slices containing the cDNAs from cleaved and uncleaved RNA fragments from the same transcription reaction were combined into a single tube and cDNAs were recovered by passive elution (Lib-1). For Lib-2, the cDNAs were synthesized as above except that the volumes used were twice as large as described, and the cDNAs were eluted by electrophoresis.

Sequencing Library Preparation. The sequencing libraries for Lib-1 were prepared by PCR using the isolated cDNAs as a template and primers PCR-F and PCR-R+Gua (for reactions with guanine) or PCR-R-Gua (for reactions without guanine) (Table S1). The amplification reactions were performed in 100 μL solutions containing 5 μL of cDNA solution and 0.5 μM each of the primers using Q5 High-Fidelity 2X Master Mix (New England Biolabs) for five cycles of 10 s at 98 °C followed by 30 s at 68 °C. The PCR products were purified by agarose gel electrophoresis using Zymoclean Gel DNA Recovery Kit (Zymo Research). The sequencing sample for Lib-2 was prepared similarly except that NEBNext Ultra II Q5Master Mix (New England Biolabs) was used in a 50 μL reaction containing 2.5 μL of cDNA solution.

Sequencing and Data Analysis. Sequencing was performed by OIST DNA Sequencing Section. Lib-1 sequencing samples (N3, N4, and N5) were mixed and sequenced on Illumina MiSeq sequencer using MiSeq Reagent Kit v3 (101 cycles, single-read) with 15% PhiX. Lib-2 samples were sequenced on Illumina HiSeq 4000 (150 cycles, paired-end) along with other indexed samples and PhiX. The sequencing data were analyzed with custom Perl scripts unless otherwise noted. First, the raw reads were filtered by NGS QC Toolkit v2.3.3[27] to remove low-quality reads that contain more than 30% base calls with Phred score (Q-score) below 20. The reads were sorted based on the index and the barcode sequences to determine the presence or absence of guanine and whether the original transcript was cleaved or uncleaved, and associated with the sequence of the randomized region.

PAGE Assay of Aptazyme Variants. Individual ribozyme variants (Table 1) were cloned in a plasmid and sequence verified. The plasmids were used as a template in PCR to generate DNA templates for *in vitro* transcription using Phusion High-Fidelity 2X Master Mix. *In vitro* transcription reactions were performed under the same conditions as described above for the aptazyme library production in 10 μL scale. Transcribed RNAs were separated by 8% denaturing PAGE and stained by SYBR Gold (Thermo Fisher Scientific). Gels were photographed using SE-6100 LuminoGraph I (ATTO) and analyzed by ImageJ 1.46r. Band intensities were normalized by the fragment size before calculating FC.

Consensus Structure Prediction. Consensus structures were predicted by RNAalifold in Vienna RNA package with the parameter setting -d2 −noLP.

■ ASSOCIATED CONTENT

Ⓢ Supporting Information

The Supporting Information is available free of charge on the ACS Publications website at DOI: 10.1021/acssynbio.7b00057.

Oligonucleotides used in this study; summary of deep sequencing statistics; guanine responsive aptazymes; Lib-2 variants with the lowest FC values; additional figures (PDF)

Data set containing ribozyme activities of all Lib-2 variants acquired by deep sequencing (XLSX)

■ AUTHOR INFORMATION

Corresponding Author

*E-mail: yohei.yokobayashi@oist.jp.

ORCID ⓘ

Yohei Yokobayashi: 0000-0002-2417-1934

Notes

The authors declare no competing financial interest.

■ ACKNOWLEDGMENTS

■ REFERENCES

(1) Felletti, M., and Hartig, J. S. (2017) Ligand-dependent ribozymes. *Wiley Interdiscip. Rev.: RNA 8*, e1395.

(2) Schlosser, K., and Li, Y. (2009) Biologically inspired synthetic enzymes made from DNA. *Chem. Biol. 16*, 311−322.

(3) Groher, F., and Suess, B. (2014) Synthetic riboswitches - A tool comes of age. *Biochim. Biophys. Acta, Gene Regul. Mech. 1839*, 964−973.

(4) Wieland, M., and Hartig, J. S. (2008) Improved aptazyme design and in vivo screening enable riboswitching in bacteria. *Angew. Chem., Int. Ed. 47*, 2604−2607.

(5) Ogawa, A., and Maeda, M. (2008) An artificial aptazyme-based riboswitch and its cascading system in E. coli. *ChemBioChem 9*, 206−209.

(6) Win, M. N., and Smolke, C. D. (2007) A modular and extensible RNA-based gene-regulatory platform for engineering cellular function. *Proc. Natl. Acad. Sci. U. S. A. 104*, 14283−14288.

(7) Kumar, D., An, C.-I., and Yokobayashi, Y. (2009) Conditional RNA interference mediated by allosteric ribozyme. *J. Am. Chem. Soc. 131*, 13906−13907.

(8) Zhong, G., Wang, H., Bailey, C. C., Gao, G., and Farzan, M. (2016) Rational design of aptazyme riboswitches for efficient control of gene expression in mammalian cells. *eLife 5*, e18858.

(9) Beilstein, K., Wittmann, A., Grez, M., and Suess, B. (2015) Conditional control of mammalian gene expression by tetracycline-dependent hammerhead ribozymes. *ACS Synth. Biol. 4*, 526−534.

(10) Wieland, M., Benz, A., Klauser, B., and Hartig, J. S. (2009) Artificial ribozyme switches containing natural riboswitch aptamer domains. *Angew. Chem., Int. Ed. 48*, 2715−2718.

(11) Kobori, S., Ichihashi, N., Kazuta, Y., Matsuura, T., and Yomo, T. (2012) Kinetic analysis of aptazyme-regulated gene expression in a cell-free translation system: Modeling of ligand-dependent and -independent expression. *RNA 18*, 1458−1465.

(12) Nomura, Y., Kumar, D., and Yokobayashi, Y. (2012) Synthetic mammalian riboswitches based on guanine aptazyme. *Chem. Commun. 48*, 7215−7217.

(13) Nomura, Y., Zhou, L., Miu, A., and Yokobayashi, Y. (2013) Controlling mammalian gene expression by allosteric hepatitis delta virus ribozymes. *ACS Synth. Biol. 2*, 684−689.

(14) Felletti, M., Stifel, J., Wurmthaler, L. A., Geiger, S., and Hartig, J. S. (2016) Twister ribozymes as highly versatile expression platforms for artificial riboswitches. *Nat. Commun. 7*, 12834.

(15) Weinberg, Z., Kim, P. B., Chen, T. H., Li, S., Harris, K. A., Lünse, C. E., and Breaker, R. R. (2015) New classes of self-cleaving ribozymes revealed by comparative genomics analysis. *Nat. Chem. Biol. 11*, 606−610.

(16) Harris, K. A., Lünse, C. E., Li, S., Brewer, K. I., and Breaker, R. R. (2015) Biochemical analysis of pistol self-cleaving ribozymes. *RNA 21*, 1852−1858.

(17) Kobori, S., Nomura, Y., Miu, A., and Yokobayashi, Y. (2015) High-throughput assay and engineering of self-cleaving ribozymes by sequencing. *Nucleic Acids Res. 43*, e85.

(18) Kobori, S., and Yokobayashi, Y. (2016) High-throughput mutational analysis of a twister ribozyme. *Angew. Chem., Int. Ed. 55*, 10354−10357.

(19) Ren, A., Vušurović, N., Gebetsberger, J., Gao, P., Juen, M., Kreutz, C., Micura, R., and Patel, D. J. (2016) Pistol ribozyme adopts a pseudoknot fold facilitating site-specific in-line cleavage. *Nat. Chem. Biol. 12*, 702−708.

(20) Nguyen, L. A., Wang, J., and Steitz, T. A. (2017) Crystal structure of Pistol, a class of self-cleaving ribozyme. *Proc. Natl. Acad. Sci. U. S. A. 114*, 1021−1026.

(21) Mandal, M., Boese, B., Barrick, J. E., Winkler, W. C., and Breaker, R. R. (2003) Riboswitches control fundamental biochemical pathways in Bacillus subtilis and other bacteria. *Cell 113*, 577−586.

(22) Garst, A. D., Edwards, A. L., and Batey, R. T. (2011) Riboswitches: structures and mechanisms. *Cold Spring Harbor Perspect. Biol. 3*, a003533.

(23) Zhu, Y. Y., Machleder, E. M., Chenchik, A., Li, R., and Siebert, P. D. (2001) Reverse transcriptase template switching: a SMART approach for full-length cDNA library construction. *BioTechniques 30*, 892−897.

(24) Diegelman-Parente, A., and Bevilacqua, P. C. (2002) A mechanistic framework for co-transcriptional folding of the HDV genomic ribozyme in the presence of downstream sequence. *J. Mol. Biol. 324*, 1−16.

(25) Chadalavada, D. M., Knudsen, S. M., Nakano, S.-i., and Bevilacqua, P. C. (2000) A role for upstream RNA structure in facilitating the catalytic fold of the genomic hepatitis delta virus ribozyme1. *J. Mol. Biol. 301*, 349−367.

(26) Lorenz, R., Bernhart, S. H., Höner zu Siederdissen, C., Tafer, H., Flamm, C., Stadler, P. F., and Hofacker, I. L. (2011) ViennaRNA Package 2.0. *Algorithms Mol. Biol. 6*, 26.

(27) Patel, R. K., and Jain, M. (2012) NGS QC Toolkit: A toolkit for quality control of next generation sequencing data. *PLoS One 7*, e30619.

(28) Crooks, G. E., Hon, G., Chandonia, J.-M., and Brenner, S. E. (2004) WebLogo: A sequence logo generator. *Genome Res. 14*, 1188−1190.